Elastic π^+-p and p-p Scattering at 1.23 Bev/c*

L. O. ROELLIG† AND D. A. GLASER
Randall Laboratory of Physics, University of Michigan, Ann Arbor, Michigan

(Received June 16, 1959)

Elastic π^+-p scattering at 1.1 Bev and elastic $p-p$ scattering at 582 Mev have been measured using a propane bubble chamber. On the basis of 661 identified π^+-p elastic scatterings found in the scanning of 1.726×10^6 cm of pion track, the total elastic cross section is found to be 12.3 ± 1.2 mb. The differential cross section is rather isotropic at large angles and exhibits a strong peak for small forward scattering angles. If the forward peak is interpreted as diffraction scattering according to the optical model, the data are best fitted by a proton with a π^+-p interaction radius, $R=(0.99_{-0.11}^{+0.13})\times10^{-13}$ cm and an opacity, $O=0.70_{-0.07}^{+0.06}$.

The total cross section for p-p elastic scattering at 582 Mev was found to be 24.2 ± 1.6 mb on the basis of 2442 elastic scatterings observed in the scanning of 3.000×10^6 cm of proton track. Both differential and total p-p cross sections are in excellent agreement with the results of counter experiments in this energy region.

I. INTRODUCTION

ALTHOUGH total and elastic π^--p cross sections are known fairly well for pion energies up to 5 Bev,[1] π^+-p cross sections are not so well known. The π^+-p total cross section is known to 1.9 Bev[2] and the elastic π^+-p cross section has been measured up to 480 Mev.[3] To extend our knowledge of the π^+-p interaction, we have measured the elastic scattering of 1.1-Bev π^+ mesons against free protons in a propane bubble chamber exposed to a 1.23-Bev/c beam of positive particles produced by the Brookhaven Cosmotron. The beam contained mainly positive pions and protons so that both π^+-p and $p-p$ scatterings were observed. These were identified and separated by our analysis procedure so that we also measured p-p elastic scattering at a proton kinetic energy of 582 ± 21 Mev. Since elastic and total p-p cross sections are known up to an energy of 9 Bev,[4,5] our p-p scattering results do not contribute much new information but serve mainly to check previous counter measurements done at 560 Mev and 590 Mev.[4] It is reassuring that the bubble chamber and the counter measurements agree excellently since the possible sources of bias and systematic error are likely to be different for the two techniques.

II. EXPERIMENTAL PROCEDURE

A. The Bubble Chamber

The Michigan propane bubble chamber,[6] which has a sensitive volume of $12\times5\times5$ inches, was used with no magnetic field for this experiment.

B. The 1.23 Bev/c Pion Proton Beam

Experimental information on π^+ scattering above 1.0 Bev was very difficult to obtain until the recent development of an intense external proton beam at the Cosmotron. Pions of energies above 1.0 Bev are produced strongly forward and if they originate in targets inside the Cosmotron, the positive ones are bent inward by the Cosmotron field and are inaccessible for observation. When the target is placed in a field-free straight section, too few of the pions are emitted at a large enough angle to get out of the machine. Positive beams of high-energy particles produced internally at 30° or 40° contain mostly protons and too few pions

* Supported in part by the U. S. Atomic Energy Commission; part of a thesis submitted by L. O. Roellig in partial fulfillment of the requirements for the Ph.D. degree at The University of Michigan.

† Now at Wayne State University, Detroit, Michigan.

[1] H. A. Bethe and F. de Hoffmann, *Mesons and Fields* (Row, Peterson and Company, Evanston, 1955), Vol. II: W. D. Walker and J. Crussard, Phys. Rev. **98**, 1416 (1955); Eisberg, Fowler, Lea, Shephard, Shutt, Thorndike, and Whittemore, Phys. Rev. **97**, 797 (1955); Maenchen, Fowler, Powell, and Wright, Phys. Rev. **108**, 850 (1957); W. D. Walker, Phys. Rev. **108**, 872 (1957); Walker, Hushfar, and Shephard, Phys. Rev. **104**, 526 (1956); A. R. Erwin and J. K. Kopp, Phys. Rev. **109**, 1364 (1958); R. C. Whitten and M. M. Block, Phys. Rev. **111**, 1676 (1958); Chretien, Leitner, Samois, Schwartz, and Steinberger, Phys. Rev. **108**, 383 (1957).

[2] Cool, Piccioni, and Clark, Phys. Rev. **103**, 1082 (1956).

[3] Morris, Rahm, Rau, Thorndike, and Willis, Bull. Am. Phys. Soc. Ser. II, **3**, 33 (1958); Blevins, Block, and Leitner, Phys. Rev. **112**, 1287 (1958).

[4] Nikitin, Selector, Bogomolov, and Zombkovskij, Nuovo cimento **2**, 1269 (1955); Smith, McReynolds, and Snow, Phys. Rev. **97**, 1186 (1955).

[5] Fowler, Shutt, Thorndike, Whittemore, Cocconi, Hart, Block, Harth, Fowler, Garrison, and Morris, Phys. Rev. **103**, 1489 (1956); Cork, Wenzel, and Causey, Phys. Rev. **107**, 859 (1957); Duke, Loch, March, Gibson, McKeague, Hughes, and Muirhead, Phil. Mag. **46**, 877 (1955); Shapiro, Leavitt, and Chen, Phys. Rev. **95**, 663 (1954); Chen, Leavitt, and Shapiro, Phys. Rev. **103**, 212 (1956); Marshall, Marshall, and Nedzel, Phys. Rev. **98**, 1513 (1955); Ypsilantis, Wiegand, Tripp, Segrè, and Chamberlain, Phys. Rev. **98**, 840 (1955); Sutton, Fields, Fox, Kane, Mott, and Stallwood, Phys. Rev. **97**, 783 (1955); Kane, Stallwood, Sutton, Fields, and Fox, Phys. Rev. **95**, 1694 (1954); Chamberlain, Segrè, Tripp, Wiegand and Ypsilantis, Phys. Rev. **93**, 1430 (1954); J. M. Dickson and D. C. Salter, Nature **173**, 946 (1954); Marshall, Marshall, and Nedzel, Phys. Rev. **93**, 927 (1953); Chamberlain, Segrè, and Wiegand, Phys. Rev. **83**, 929 (1951); "Russian Experiments with 660-Mev Synchrocyclotron," Argonne National Laboratory, 1955, translated by M. Hamermesh from Doklady Akad. Nauk U. S. S. R., 99, No. 6 (1954); O. Piccioni, 1958 Annual International Conference on High-Energy Physics at CERN, edited by B. Ferritti (CERN Scientific Information Service, Geneva, 1958), p. 74.

[6] J. Brown, Ph.D. thesis, The University of Michigan, 1958 (unpublished).

for scattering measurements using present techniques.

When the pions are produced by the external proton beam striking a target outside the Cosmotron ring, a beam of resonable pion intensity can be obtained by selecting particles emerging from the target near the forward direction. The actual beam set-up was based on the results of an earlier experiment which showed that the p/π ratio decreases with decreasing atomic number of the target material, decreasing pion momentum, and decreasing production angle.[7] Figure 1 is a floor plan of the arrangement. On striking a $1\times1\times6$ inch polyethylene target at T, the 3-Bev external proton beam produces a spectrum of pions in all directions. Since energetic pions are produced mainly in the forward direction, strong focussing magnetic quadrupoles H and J were set up to accept a solid angle centered about a line making an angle of 7° with respect to the external proton beam direction. A 3×3-inch collimator at (a) limited the acceptance angle of the quadrupole to avoid pole-face scattering, and that part of the primary beam not absorbed in the target was dissipated in the lead walls of the collimator and in the iron of magnet H. These focussing magnets were adjusted to form an image of the target on the 1×1-inch collimator at (c). Momentum analysis was provided by magnet B which deflected the beam through an angle of 23°. From the known quadrupole characteristics the target image at (c) was calculated to be 0.92 inch wide,[8] and a momentum resolution of $\pm0.75\%$ was predicted. Counter measurements of the beam width checked these calculations. Taking into account fluctuations in magnet currents observed during the experiment, the actual momentum of the beam used was 1.232 Bev/$c\pm1.5\%$. Such good momentum resolution is important because events are identified mainly on the basis of kinematics. To reduce broadening of the target image due to multiple scattering in air a helium-filled plastic bag was inserted between magnet and the collimator at (c). Magnet E was used to sweep

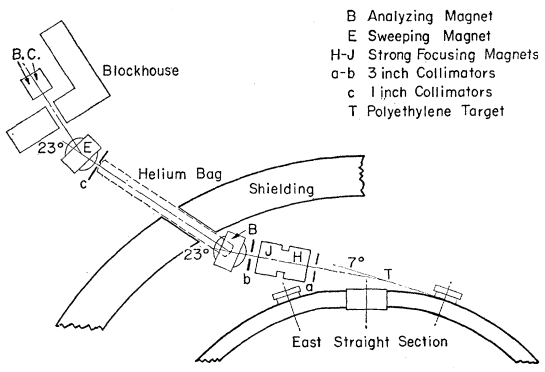

FIG. 1. Experimental layout.

[7] Brookhaven National Laboratory Report CCD-1 (unpublished).

[8] Brookhaven National Laboratory Report RMS-55 (unpublished).

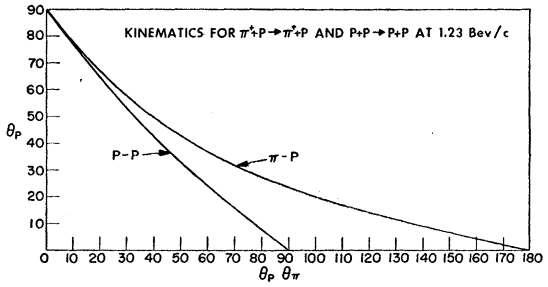

FIG. 2. Kinematics for $\pi^+ + p \rightarrow \pi^+ + p$ and $p+p \rightarrow p+p$ at 1.23 Bev/c.

out of the beam the unwanted low momentum particles coming from the collimator. Finally the beam passed through the bubble chamber (B.C.), which was shielded from the general room background by a house of concrete blocks.

The p/π ratio of the beam was measured by a time-of-flight technique similar to that used by Cool, Piccioni, and Clark[2] and found to be 1.75 ± 0.09. Previous measurements of similar beams lead to the estimate that the muon contamination was less than $(8\pm3)\%$ and the electron contamination less than 1% of the pion intensity.

III. DATA REDUCTION

A total of 234 000 tracks was scanned for elastic scatterings of positive pions and protons by free protons. Approximately 10 000 two-prong stars were found which looked like elastic scatterings. These events were measured, and the geometry of each event computed by an IBM-650 computer. A geometrical error depending on the particular configuration of the event was also computed for all of the various track lengths and angles associated with the scattering.

Elastic $\pi^+ - p$ and p-p scatterings were identified by the following methods: angular correlations; coplanarity; range; bubble density, and δ rays produced by the beam track. Figure 2 contains the kinematic curves for the reactions $\pi^+ - p \rightarrow \pi^+ + p$ and $p+p \rightarrow p+p$. Notice that for small angle scatterings it is not possible to distinguish a $\pi^+ - p$ elastic scattering from a p-p elastic scattering. Because each event has its own peculiar geometrical error, it is not possible to state in general how small the angle of a scattering can be and still allow a $\pi^+ - p$ event to be distinguished from a p-p event. The lower limit was usually about 17°. As seen in Fig. 3 the coplanarity of identified inelastic events is peaked around small angles due to the high energy of the incoming beam. For this reason the coplanarity criterion could be used only to reject two prong stars as elastic events rather than identify them as elastic scatterings. The range of the proton is plotted as a function of its angle in Fig. 4. Range measurements provides a sensitive criterion for distinguishing elastic events from inelastic events, but it loses its usefulness

for separating small angle elastic π^+-p scatterings from small-angle elastic p-p scatterings, i.e., when θ_p is large. The bubble density of the scattered tracks had to be consistent with the bubble density one would expect from kinematic considerations before an apparent scattering was accepted as a true scattering. Bubble density observations are especially useful in rejecting apparent π^+-p scatterings, for at all scattering angles (including directly backwards, i.e., $\theta_\pi=180°$) the pion track must be light. About 10% of the apparent π^+-p scatterings were rejected because the pion track was not light. δ rays produced by the beam particles were used to differentiate π^+-p elastic scatterings from p-p elastic scatterings when the above four criteria were unable to do this. For a few of the large-angle scatterings separation of π^+-p and p-p events was difficult. This happened when the scattering had a peculiar geometry which could cause a large angular error, e.g., when the scattered particle scattered a second time close to the vertex of the first scattering. In these cases, the measureable track length of the scattered particle is short, and hence the error in the angular measurement could be large. The use of δ rays to distinguish π beam tracks from p beam tracks is based upon the fact that for a given momentum a π meson can impart more energy to a struck electron than a proton can. The maximum energy a 1.19-Bev/c proton (the momentum of the proton in the center of the bubble chamber) can give an electron is 1.66 Mev, whereas the maximum energy a 1.23-Bev/c pion can give an electron is 74.5 Mev. By means of an expression derived by Bhabha it was calculated that the cross section of a 1.23-Bev/c pion for producing a δ ray with 1.66 Mev$\leq E\leq$74.5 Mev in propane is 3.62×10^{-24} cm^2.[9] This calculation was experimentally checked by counting δ rays with an energy greater than 1.66 Mev along identified pion tracks. By scanning the beam tracks that terminated in an unidentified elastic scattering and counting those δ rays of energy greater than 1.66 Mev produced along those tracks, it was possible to calculate the total length of pion track scanned by using the above cross section for high-energy δ-ray production. Since the mean free path for the beam protons and pions is long with respect to the length of the chamber,

$$N_\pi/N_t=L_\pi/L_t,$$

where N_π=number of pions in the group of undecided elastic scatterings, N_t=total number of undecided elastic scatterings, L_π=calculated length of pion track scanned based upon the number of δ rays found, and L_t=total length of beam track scanned which terminated in an undecided elastic scattering.

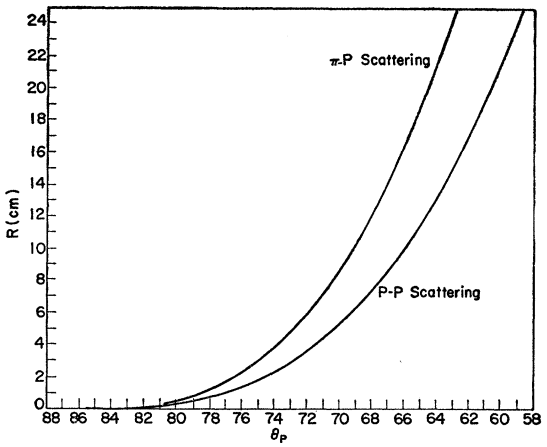

FIG. 4. The range of the proton for π^+-p and $p-p$ scatterings at 1.23 Bev/c as a function of the proton angle.

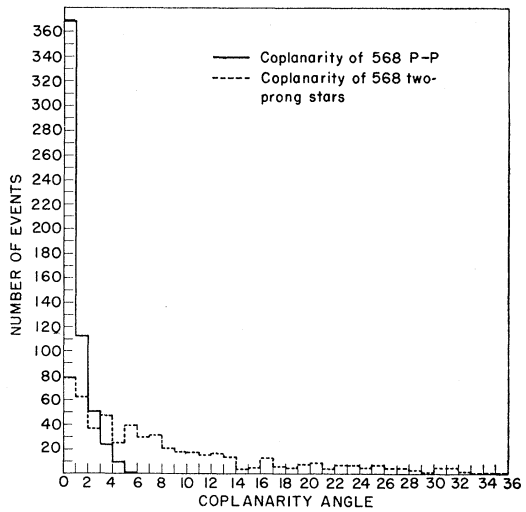

FIG. 3. Coplanarity histogram.

[9] H. J. Bhabha, Proc. Roy. Soc. (London) **A164**, 257 (1938).

IV. ERRORS, BIASES, AND CONTAMINATIONS

A. Scanning and Measurement

1. Absolute Scanning Efficiency

Each picture was scanned by at least two different scanners in order to increase the total scanning efficiency for the experiment and to obtain the scanning efficiency of the individual scanners. Assuming that all events are equally difficult to find, the method used to obtain the scanning efficiency based upon the rescanning is as follows: Let

N_1=number of events scanner 1 finds,

N_2=number of events scanner 2 finds,

N_{12}=number of events scanners 1 and 2 find in common,

N=true number of events in the pictures scanned,

e_1=scanning efficiency of scanner 1, and

e_2=scanning efficiency of scanner 2.

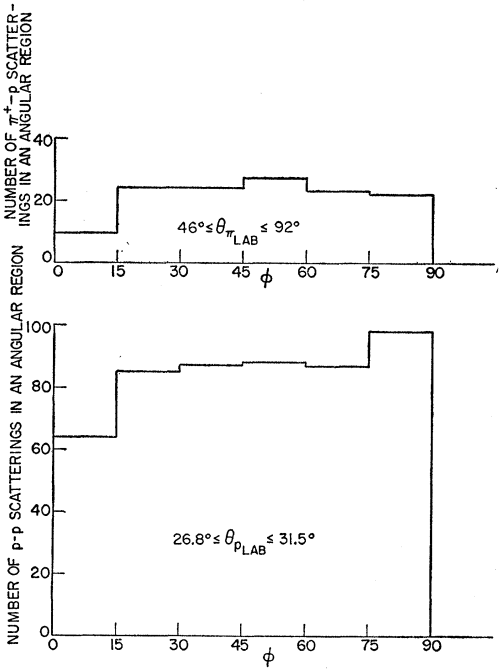

FIG. 5. Representative histograms used for the azimuthal corrections.

Then

$$N_1 = e_1 N,$$
$$N_2 = e_2 N,$$
$$N_{12} = e_1 e_2 N.$$

Therefore

$$e_1 = N_{12}/N_2,$$
$$e_2 = N_{12}/N_1,$$

and the total scanning efficiency is given by

$$\text{total efficiency} = 1-(1-e_1)(1-e_2).$$

Using this method the total scanning efficiency was found to exceed 99%.

2. *Relative Scanning Efficiency*

In the analysis above we assumed that all events are equally difficult to find, but actually small-angle scatterings in which the plane of the scattering is parallel to the camera line of sight are more easily missed than large-angle scatterings whose plane is perpendicular to the line of sight. To test whether the scanning efficiency was uniformly lower for the "difficult" configurations, all identified elastic scatterings were divided into eight groups according to their scattering angles. For each group of scatterings a histogram was made which correlated the azimuthal angles of the scattering to number of scatterings for each azimuthal increment. Two representative histograms are shown in Fig. 5. An azimuthal angle of $\phi=0°$ corresponds to the scattering plane being parallel to the line of sight, and $\phi=90°$ corresponds to the scattering plane being perpendicular to the line of sight. The columns in each histogram should be of equal height because of the manner in which the azimuthal angle was computed, i.e., $0° \leq \phi \leq 90°$ rather than $0° \leq \phi \leq 360°$. It can be seen that a differential azimuthal scanning bias does exist, indicating there were classes of events in which the scanning efficiency was uniformly lower than for other classes. On the basis of these graphs, a differential scanning efficiency was then computed. It was found that the relative scanning efficiency depended upon the scattering angle as well as the aximuthal angle of scattering. The differential scanning efficiency varied from 88% for pions scattered in the backward direction to 98% for wide-angle proton scatterings.

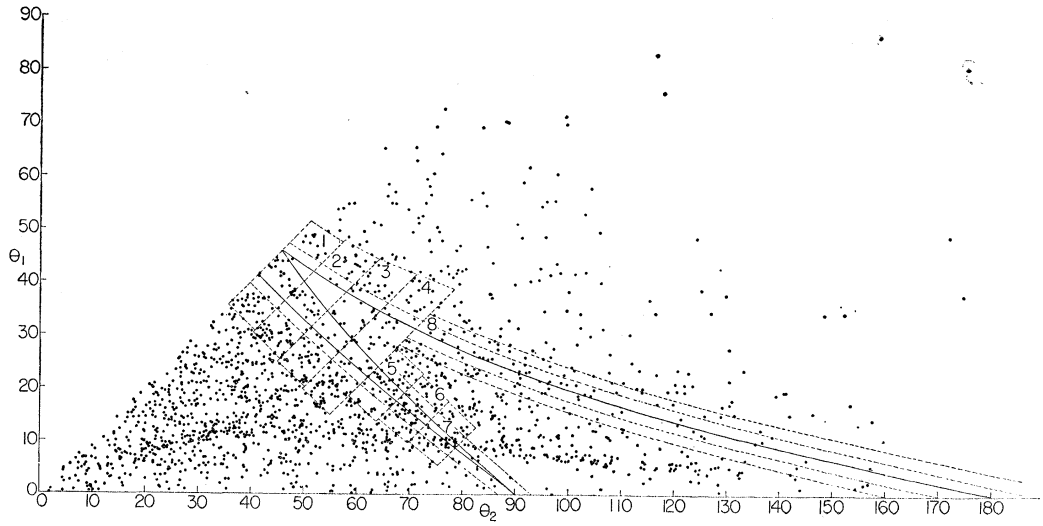

FIG. 6. Coplanar carbon events.

TABLE I. Corrections to the π^+-p cross sections.

Interval $\cos\theta_{c.m.}$	Azimuthal correction	Muon contamination	Beam attenuation	Measuring efficiency	Carbon contamination	C[a]
0.91– 0.8	0.98±0.5%	0.92±3%	0.91±1%	0.94±2%	1.01±3%	1.31±5%
0.8 – 0.6	0.97±0.5%	0.92±3%	0.91±1%	0.94±2%	0.88±2%	1.15±4%
0.6 – 0.4	0.97±0.5%	0.92±3%	0.91±1%	0.94±2%	0.88±2%	1.15±4%
0.4 – 0.2	0.88±4%	0.92±3%	0.91±1%	0.94±2%	0.88±2%	1.27±6%
0.2 – 0.0	0.88±4%	0.92±3%	0.91±1%	0.94±2%	0.88±2%	1.27±6%
0.0 ––0.2	0.88±4%	0.92±3%	0.91±1%	0.94±2%	0.88±2%	1.27±6%
−0.2 ––0.4	0.88±4%	0.92±3%	0.91±1%	0.94±2%	0.89±2%	1.28±6%
−0.4 ––0.6	0.88±4%	0.92±3%	0.91±1%	0.94±2%	0.89±3%	1.28±6%
−0.6 ––0.8	0.89±4%	0.92±3%	0.91±1%	0.94±2%	0.89±3%	1.27±6%
−0.8 ––1.0	0.89±4%	0.92±3%	0.91±1%	0.94±2%	0.89±3%	1.27±6%

[a] C is the total correction that must be added to the raw-data cross section, where C = (carbon contamination)/[(measuring efficiency)(azimuthal correction)(beam attenuation)(muon contamination)].

3. *Measurement*

Approximately 4% of the scatterings measured were remeasured to determine error rate of the measuring process. Two measurements of an event were considered to agree when the corresponding computed quantities (ϕ, θ_1, θ_2, etc.) of each measurement differed by no more than the sum of their errors. By this method 94±2% of the events were found to have been measured correctly.

B. Carbon Contamination

Since approximately two-thirds of the total number of protons in the chamber are protons bound in carbon, the possibility that some of the accepted events might be grazing collisions in carbon, rather than collisions with free protons, must carefully be considered. To obtain an estimate of the number of such quasi-elastic events produced in carbon, 1748 two-prong stars, which satisfied the coplanarity criteria but which were not identified as elastic scattering, were studied. See Fig. 6. Since in most cases it is impossible to tell pion tracks from proton tracks, the larger angle has been plotted against the smaller. The upper parts of the π^+-p and p-p kinematic curves have been folded over about the line $\theta_1=\theta_2$.

The contamination of carbon events is determined by plotting all the coplanar carbon events on a graph of the π^+-p and p-p elastic scattering angular kinematic curves and assuming that the density of the coplanar carbon events varies linearly in the region of the angular kinematic curves. Then if one has identified coplanar carbon events on or near the angular kinematic curve as "good" events, the density of the coplanar carbon events will be lower in this region than it is in adjacent regions. Tables I and II summarize the contamination estimates.

C. Incident Beam Intensity

By counting incoming beam tracks in every twentieth picture, the total number of tracks scanned is found to be 234 000±1.6%. There were 25 tracks per picture on the average.

D. Beam Attenuation

Because the beam particles are counted as they enter the bubble chamber to obtain the total length of beam scanned, a calculation has to be made to determine the attenuation of the beam in the chamber due to its interaction with the propane.

The total $p-$C, p-p, π^+-C, and π^+-p cross sections have been measured at the momentum of this experiment.[2,4,10] They are

$$\sigma_{t(\pi-p)}=29\pm3 \text{ mb}, \quad \sigma_{t(p-p)}=25\pm2 \text{ mb},$$
$$\sigma_{t(\pi-C)}=240 \text{ mb}, \quad \sigma_{t(p-C)}=340\pm10 \text{ mb}.$$

From these cross sections the attenuation of the proton is found to be 11%±1%, and that of the pion beam 9%±1%.

V. EXPERIMENTAL RESULTS

A. π^+-p Elastic Scattering

The differential cross section for elastic scattering is computed by applying the product of the correction factors discussed in Sec. IV to the uncorrected data

$$\frac{d\sigma}{d\Omega}=\frac{C}{Nx}\frac{dn}{d\Omega}=C\left(\frac{d\sigma}{d\Omega}\right)_{\text{uncorrected}}. \quad (1)$$

Here $N=4.87\times10^{22}$ cm^{-3} is the number of protons per cubic centimeter of propane, $x=1.726\times10^6$ cm is the total length of pion track scanned, dn is the number of

TABLE II. Corrections to the p-p cross sections.

Interval $\theta_{c.m.}$, deg	Azimuthal correction	Measuring efficiency	Beam attenuation	Carbon contamination	c[a]
30–40	0.99 ±0.5%	0.94±2%	0.89±1%	1.02±1%	1.23±2.5%
40–50	0.97 ±0.5%	0.94±2%	0.89±1%	1.01±1%	1.25±2.5%
50–60	0.985±0.5%	0.94±2%	0.89±1%	0.98±1%	1.18±2.5%
60–70	0.96 ±0.5%	0.94±2%	0.89±1%	0.98±1%	1.22±2.5%
70–80	0.98 ±0.5%	0.94±2%	0.89±1%	0.96±1%	1.17±2.5%
80–90	0.98 ±0.5%	0.94±2%	0.89±1%	0.97±1%	1.18±2.5%

[a] C = (carbon contamination)/[(measuring efficiency)(azimuthal correction)(beam attenuation)].

[10] V. I. Moskalev and B. V. Gavrilovskiĭ, Doklady Akad Nauk U. S. S. R. **110**, 972 (1956) [translation: Soviet Phys. Doklady **1**, 607 (1956)].

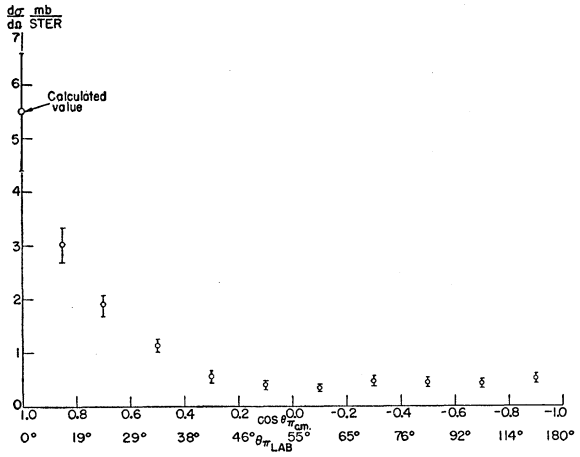

FIG. 7. π^+-p differential cross section at 1.1 Bev.

pions observed to scatter into the solid angle $d\Omega$, and C is the product of correction factors discussed in Sec. IV. In Table I are given the relevant factors as a function of the center-of-mass scattering angle of the π^+.

Figure 7 is a plot of the differential cross section *versus* angle of scattering of the π^+ in the center-of-mass and laboratory systems.

Since the scattering cross section is large in the forward direction where measurements are difficult, the total elastic cross section cannot be obtained directly from our data with high accuracy. We therefore make use of the "optical theorem" which relates the imaginary part of the coherent forward scattering amplitude to the total (elastic and inelastic) interaction cross section:

$$\mathrm{Im}f_c(0°)=k\sigma_t/4\pi. \quad (2)$$

Cool, Piccioni, and Clark[2] find $\sigma_t=28.8\times10^{-27}$ cm^2 $\pm10\%$ and $k=3.25\times10^{13}$ cm^{-1} for 1.23-Bev/c pions. This gives $[\mathrm{Im}f_c(0°)]^2=(5.54\pm1.1)\times10^{-27}$ cm^2. Since Sternheimer[11] has shown by the use of dispersion relations that $R_ef_c(0°)=0$, the coherent part of the forward elastic differential cross section is

$$\frac{d\sigma_c}{d\Omega}(0°)=[R_ef_c(0°)]^2+[\mathrm{Im}f_c(0°)]^2$$
$$=(5.5\pm1.1)\ \mathrm{mb/sterad}. \quad (3)$$

Since the spin-flip cross section vanishes at 0°, this is just the total forward elastic cross section.

B. p-p Elastic Scattering

From the 3.000×10^6 cm of proton track scanned the differential elastic p-p scattering cross section is found in the same way. The results are tabulated in Table II and plotted in Fig. 8 along with the results of two counter measurements at neighboring energies. The close agreement among the three experiments is most reassuring.

To obtain the total p-p elastic cross section, the differential cross section was plotted *versus* $\cos\theta_{\mathrm{cm}}$ and a linear extrapolation to forward angles carried out. The total elastic cross section for p-p scattering at 582 ± 21 Mev was found to be 24.2 ± 1.6 mb, in excellent agreement with Smith's[4] value of 25 ± 2 mb at 590 ± 15 Mev.

VI. INTERPRETATION OF THE DATA

It can be seen in Fig. 7 that the angular distribution of π^+-p elastic scattering has the same general features as are observed for π^--p scattering in the same energy range.[1] The large forward peak can be interpreted as dominantly diffraction scattering which can be fitted quite well by the optical model.[12] At the backward angles the more or less isotropic angular distribution has been attributed by some authors to incoherent elastic scattering resulting from the formation of a pion-proton compound system which decays isotropically and with random phase with respect to the incident pion beam.[13] Attempts to explain the backward distribution by a phase-shift analysis or proton structure analysis have been inconclusive, although more accurate and extensive measurements may lead to useful results of this type.

By subtracting from the observed differential cross section an isotropic incoherent cross section of 0.4 mb/steradian, we find the total diffraction cross section to be 7.2 ± 0.8 mb. Using the total cross section obtained by Cool *et al.*,[2] we find the absorption cross section

$$\sigma_a=\sigma_t-\sigma_d=28.8\ \mathrm{mb}-7.2\ \mathrm{mb}=21.6\ \mathrm{mb}.$$

The inelastic cross section is

$$\sigma_i=\sigma_t-\sigma_e=28.8\ \mathrm{mb}-12.3\ \mathrm{mb}=16.5\ \mathrm{mb}.$$

In the simplest form of the optical model the absorption and diffraction cross sections are calculated from the radius of the absorbing sphere, the mean free path absorption in the sphere, and the real part of the

TABLE III. Experimental values for the interaction radius and opacity of the proton.

Type interaction	Bombarding energy (Bev)	Interaction radius in fermis (10^{-13} cm)	Opacity	Reference
π^+-p	1.1	$0.99_{-0.11}{}^{+0.13}$	$0.70_{-0.07}{}^{+0.06}$	This experiment
π^--p	1.4	1.18 ± 0.10	0.61 ± 0.10	a
π^--p	1.85	$0.85_{-0.03}{}^{+0.09}$	$0.9_{-0.2}{}^{+0.1}$	b
π^--p	5	0.9 ± 0.15	0.6 ± 0.2	c

[a] See reference 13.
[b] R. C. Whitten and M. M. Block, Phys. Rev. **111**, 1676 (1958).
[c] Maenchen, Fowler, Powell, and Wright, Phys. Rev. **108**, 850 (1957).

[11] R. M. Sternheimer, Phys. Rev. **101**, 384 (1956).

[12] Fernbach, Serber, and Taylor, Phys. Rev. **75**, 1352 (1949).

[13] Eisberg, Fowler, Lea, Shephard, Shutt, Thorndike, and Whittemore, Phys. Rev. **97**, 797 (1955).

index of refraction. This latter is defined as the ratio of the magnitude of the propagation vector inside the interacting sphere to that outside. If we assume that there is no potential scattering, so that the real part of the index of refraction is unity, we can use the curves of Bethe and Wilson[14] to determine the radius of the pion-proton interaction from our measured values of σ_a and σ_d. In this way we find the radius of the proton to be $(0.99_{-0.11}{}^{+0.13})\times10^{-13}$ cm and its opacity $\sigma_a/\pi R^2 = 0.70_{-0.07}{}^{+0.06}$. Substituting this value of the proton radius in the angular distribution predicted by Fernbach, Serber, and Taylor we find good agreement with our measured angular distribution.

In Table III a comparison is made of the values of the proton radius and opacity obtained by our π^+ scattering observations and others found by π^--p scattering near 1 Bev.

To compare the "electromagnetic" proton radius found at Stanford by electron scattering with the "pionic" radius, we should express our result in terms of a root-mean-square radius for the optical model. The pionic value of the root-mean-square radius of the proton from this experiment is $(0.77_{-0.09}{}^{+0.10})\times10^{-13}$ cm, while for the electromagnetic radius Chambers and Hofstadter find $(\langle r^2\rangle_{\text{Av}})^{\frac{1}{2}} = (0.77\pm0.10)\times10^{-13}$ cm.[15]

VII. CONCLUSIONS

A total of 1.726×10^6 cm of pion track and 3.000×10^6 cm of proton track was scanned for elastic π^+-p interactions at 1.1 Bev and elastic p-p interactions at 582 Mev. This is the first π^+-p elastic scattering in the Bev region to be reported, whereas the p-p elastic scattering has already been measured in this energy region, so the p-p data will serve mainly to show that there was no large systematic bias in the previously reported counter experiments or in this experiment, since the biases are not likely to be identical.

On the basis of 661 identified π^+-p elastic scatterings the total elastic cross section and the angular distribution of the differential cross section were measured. The total elastic cross section was found to be 12.3 ± 1.2 mb. The angular distribution of the differential cross section was found to exhibit a peaking for small-angle scattering and a rather isotropic distribution for large-angle scattering. The optical model was then applied to the experimental data, and a proton interaction radius of $R=(0.99_{-0.11}{}^{+0.13})\times10^{-13}$ cm was found to fit the data by two independent methods of calculation. The opacity of the proton was found to be $O=0.70_{-0.07}{}^{+0.06}$.

A total of 2442 elastic p-p scatterings was observed. From these data a total cross section of 24.2 ± 1.6 mb was calculated. The angular distribution of the p-p elastic differential cross section was found to agree with that previously reported by counter experiments in this energy region.

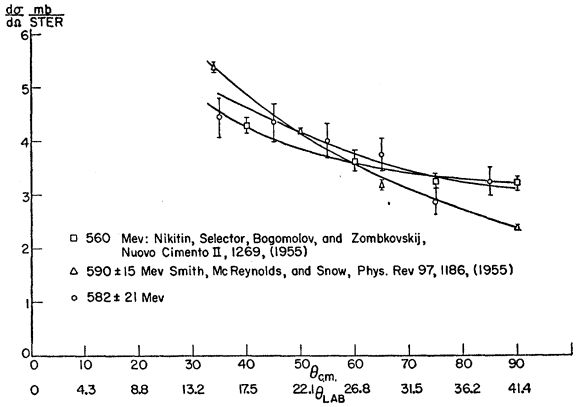

FIG. 8. p-p differential cross section at about 600 Mev.

VIII. ACKNOWLEDGMENTS

It is a pleasure to acknowledge the aid of Dr. John Brown, Dr. James Cronin, Dr. Martin Perl, and Dr. John Vander Velde in planning and running this experiment. We would also like to extend our thanks to: the Cosmotron group; Richard Hartung, who programed the IBM-650 computer; and Dolores Moebs, Elsie Brown, Vivian French, and Pauline Roellig who assisted in scanning the film and performing the measurements.

[14] H. A. Bethe and R. R. Wilson, Phys. Rev. **83**, 690 (1951).
[15] E. E. Chambers and R. Hofstadter, Phys. Rev. **103**, 1454 (1956).